Synthesis of a Novel Fuel Additive Solketal Levulinate by using MOF ZIF-8 and SSA Loaded PVA Functional Catalytic Membrane

Nazli Yuzer[1], *Nilufer Hilmioglu*[1]*

[1]Chemical Engineering Department of Kocaeli University, İzmit, Kocaeli, Turkey

* Corresponding author. Chemical Engineering Department of Kocaeli University, İzmit, Kocaeli, Turkey

*E-mail address: niluferh@kocaeli.edu.tr

Graphical abstract

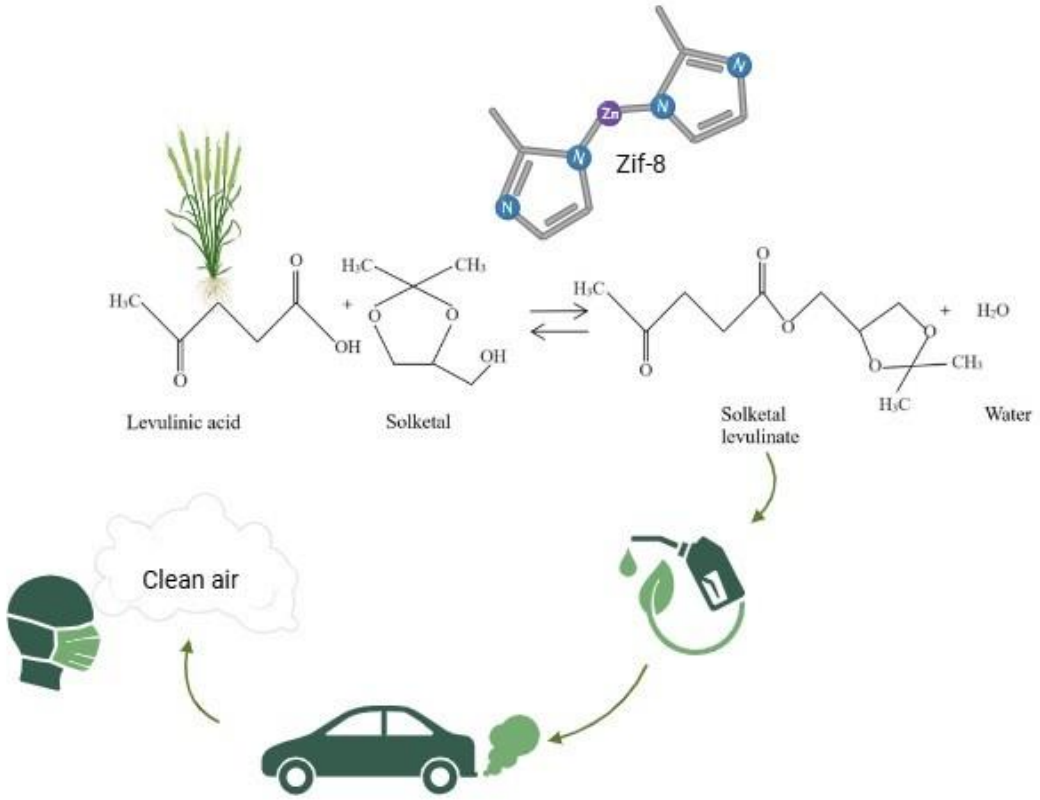

Abstract

Solketal levulinate (SoLE), a potential fuel additive that can improve the physicochemical properties of the fuel, was produced by the developed catalytic membrane from solketal and levulinic acid. The catalytic membrane was prepared in film form as a metal-organic framework of ZIF-8 supported on a sulfosuccinic acid-loaded hydrophilic polyvinyl alcohol polymer. Removing by-product water from the reaction medium with the sorption of the highly hydrophilic membrane contributed to the

conversion. PVA/SSA and PVA/SSA/ZIF-8 membranes were analyzed by FTIR and TGA. ZIF-8 was photographed and analyzed by SEM and XRD, respectively. Higher water affinity of the functional catalytic membranes was calculated by swelling degree and interaction parameter calculations. SoLE synthesis was conducted in the batch reactor under mild conditions. The parameters such as catalyst amount, temperature, solketal/levulinic acid initial molar ratio (M), and reaction time, were investigated. The PVA/SSA catalytic membrane showed a maximum reaction conversion of 97.65% with 105°C, 9 mmol SSA, and an M:6/1 ratio for 6 h. For the PVA/SSA/ZIF-8 catalytic membrane, maximum reaction conversion of 96.81% was obtained at 105°C, with an M:6/1 ratio and 9 mmol SSA for 4 hours. ZIF-8 reduced the reaction time and contributed to the system in terms of efficient energy use.

Keywords: Esterification**,** levulinic acid, heterogeneous catalyst, Bio-additive

1. Introduction

The need for energy reserves in the world is rapidly increasing in direct proportion to the growing human population. Fossil fuel reserves are in danger of exhaustion, which has increased the search for alternative fuels to satisfy energy needs. Interest in the development of green(clean)-content fuels has increased at the outset of a wide range of studies in this direction, as they are both environmentally friendly and renewable resources (Singh et al., 2023). The major problem related to combustion events of bio-based and green-content fuels, which are frequently investigated in the literature, is a key focus of research. Whether the fuels/fuels additive are fossil or green and sustainable fuels, the production of new generation fuel additives to improve the combustion properties of these fuels is an important step towards solving this problem. Toxic emissions from the combustion of fuels are reduced by optimizing engines and equipment, using catalytic converters, NOx reducers, and particulate filters for engine-based uses, as well as modifications to the chemical composition of the fuels (Çakmak and Özcan, 2018). In addition to conventional methods (isomerization, catalytic cracking, reforming-dehydrocyclization), oxygen-rich fuel additives and oxygenates can be added to improve the octane number of gasoline and the cetane number of diesel. However, traditional methods

ACCEPTED MANUSCRIPT

are costly and difficult. The octane number of gasoline or the cetane number of diesel are improved by adding oxygenates such as oxygenated alcohols and ethers after the refining of crude oil (Demirbas et al., 2015). Bio-ethanol, which is the leading bio-based fuel additive, can be obtained chemically or through fermentation. However, in both situations, long-term production processes cause both carbon emissions and system costs to increase. This makes the production process less environmentally friendly (Mussatto et al., 2010). Commonly encountered levulinate-based oxygenates in the literature include ethyl levulinate, methyl levulinate, and SoLE. However, these levulinate-based fuel additives are mainly produced by the reaction of alcohols or ketals with oxo-carboxylic acid anions (methyl levulinate, ethyl levulinate, etc.) (Jia et al., 2020). In such reactions, alcohols are used as reactants or as by-products, and these alcohols (except ethanol) are highly toxic and ecologically hazardous (Xu et al., 2020). Solketal levulinate (SoLE) is a potential levulinate-based fuel additive that improves the cold flow properties of the fuel (Mariam et al., 2024; Mariam et al., 2021). As shown in Fig. 1, SoLE can be synthesized from solketal and levulinic acid (Sutinno, 2016). This reaction, levulinic acid esterification, is a very environmentally friendly reaction in terms of both reactants and products. In addition, it produces no harmful waste. There are very few studies in the literature on the synthesis of SoLE from solketal and levulinate esters. In this study, SoLE was synthesized from solketal and levulinic acid for the first time. Levulinic acid (LA), a 5-carbon ketoacid, is one of the twelve platform chemicals defined by the US Department of Energy that can be produced from biomass; an environmentally friendly alternative to petroleum-based chemical production (Jeanmard et al., 2025). There are numerous commercial chemicals produced from LA, such as aminolevulinic acid (DALA), diphenolic acid (DPA), methyl tetrahydrofuran, various esters, and resins. Fuel additives can also be synthesized from LA, a highly versatile building block chemical. (Sajid et al., 2021; Ethiraj et al., 2022). Solketal, which is also used as a reactant in its synthesis, is a renewable and green solvent and can be used alone as an environmentally friendly fuel additive (Fernández et al., 2019; Ilgen et al., 2017). Polyvinyl alcohol (PVA) is a highly hydrophilic, biocompatible, environmentally friendly, functional synthetic polymer that can form good films. Due to its high hydrophilicity in reactions

ACCEPTED MANUSCRIPT

where water is a by-product, PVA can provide sorption support to the reaction to remove the by-product and direct the reaction equilibrium to the product side (Song et al., 2023; Unlu and Hilmioglu, 2019). Sulfosuccinic acid (SSA), which can be bio-based and sustainable, is a highly effective catalyst when added to the catalytic membrane, especially in esterification reactions due to its acidic nature (Portillo Perez et al., 2023). Zeolitic imidazolium framework-8 (ZIF-8), used as a support material in the catalytic membrane, is a type of metal-organic framework (MOF). MOFs are porous materials comprised of organic ligands and metal ions. They can be used as catalyst supports with their high specific surface area, microporosity, and finely tunable chemical and physical properties (Doan et al., 2025; Wi´sniewska et al., 2023; Laeim et al., 2025). Catalytic membranes, which are environmentally friendly functional catalysts, often composed of polymeric matrices and catalysts, are bifunctional materials that direct the reaction equilibrium towards product formation by removing the by-product of the reaction through sorption support (Hasirci et al., 2023). Studies on the synthesis of SoLE are very limited in the literature, and the synthesis was carried out by a transesterification reaction using a base catalyst. Mariam et al., 2021 synthesized SoLE from solketal and methyl levulinate as a potential fuel additive for palm biodiesel. They achieved a maximum yield of 74.83% at 140°C and 1.5% catalyst loading with Methyl levulinate/Solketal at a molar ratio of 1:4 for 6 hours. Liu et al., 2024, produced methyl levulinate glycerol ketal from methyl levulinate and glycerol. The influence of different parameters on methyl levulinate glycerol ketal yield and glycerol conversion were investigated. The optimum conditions were determined as temperature T = 140 °C, catalyst loading of 0.50 g HZSM-5, and ML/GLY mol ratio of 4:1. Under these conditions, glycerol conversion was 97%, and methyl levulinate glycerol ketal yield was 94.7%. SoLE can be manufactured by acid-catalyzed esterification of solketal and levulinic acid (Mariam et al., 2021; Sutinno, 2016). Esterification reactions are processes in which water is produced as a by-product (Moradi et al., 2021). Water removal from the reaction medium shifts the equilibrium towards the products and increases the reaction conversion (Hilmioglu, 2022). For the first time in the literature, SoLE was synthesized from solketal and levulinic acid in a batch reactor using a catalytic membrane. Blending

ACCEPTED MANUSCRIPT

catalysts used in the reaction with suitable polymer solutions to convert them from homogeneous to heterogeneous form is an excellent way to produce catalytic membranes. In this study, ZIF-8, used as a support material with an MOF cage structure was synthesized, functionalized with sulfosuccinic acid (SSA) with high Brönsted acid sites, and blended with PVA polymer to prepare catalytic membranes. In the context of SoLE production, green catalytic membranes have not been used in the literature before. Reactions with catalytic membranes are hybrid systems in which both the reaction with the catalyst and the separation of the desired product or by-product, according to the properties of the membrane material used (hydrophilic or hydrophobic), from the environment can be performed simultaneously in a single unit. For this reason, the contribution of this research article, to the literature, is promising for future studies.

This study established an experimental batch reactor system by placing catalytic membrane pieces inside. Ease of operation and re-use of the catalyst is enabled by the batch reactor, in which the reaction and sorption of the by-product occur simultaneously. This shifts the reaction balance towards the product and increases conversion without using extra reactants. The reaction was shown in Fig. 1

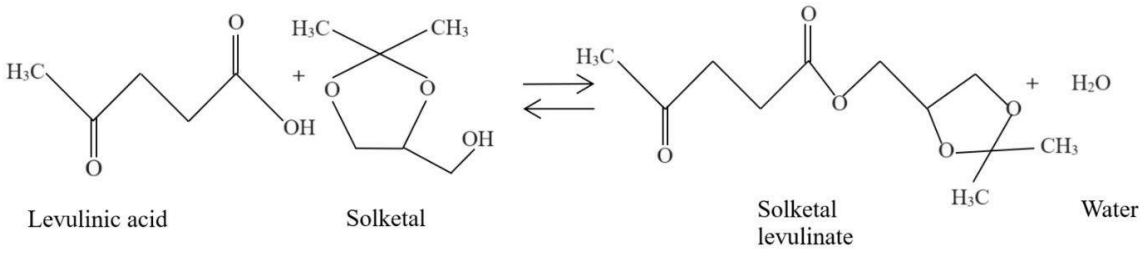

Fig. 1 Solketal levulinate synthesis from Levulinic acid and Solketal (Sutinno, 2016)

2. Materials and Methods

2.1. Materials

PVA in solid form (MW~125,000), SA (70% in water), and 2-methylimidazole were obtained from Sigma-Aldrich; zinc nitrate hexahydrate ($Zn(NO_3)_2$-$6H_2O$) was obtained from Acros Organics, while LA (for synthesis) was obtained from Merck Chemicals. Solketal was purchased from BLD Farm.

2.2. ZIF-8 synthesis

ZIF-8 was synthesized by the rapid addition of an aqueous solution of Zn $(NO_3)_2 \cdot 6H_2O$ to an aqueous solution of 2-methylimidazole. Firstly, 1.17 g of zinc nitrate was dissolved in 8 g of distilled water. Then, 22.70 g of 2-methylimidazole was dissolved separately in 80 g of distilled water. These two solutions were combined and stirred at room temperature until a turbid solution was formed. It was then centrifuged, and the ZIF-8 precipitate obtained was dried at 80 °C overnight (Pan et al., 2011).

2.3. Preparation of PVA/SSA and PVA/SSA/ZIF-8 Functional Catalytic Membranes

3, 6, and 9 mmol of SSA were added respectively to 6% PVA solutions, each prepared in certain predetermined amounts. The PVA-catalyst mixture was stirred for 1 hour and then poured onto Teflon plates and was left to dry. The dried membranes were then heat treated at 120 °C for 1 hour for crosslinking. For the preparation of ZIF-8 doped PVA/SSA membranes, 0.1 g ZIF-8 was added to PVA solutions. After stirring the PVA-ZIF-8 mixture for 1 hour, either 3, 6, or 9 mmol of SSA were added, and the mixture was further stirred. In the last step, PVA/ZIF-8/SSA mixtures were poured onto Teflon plates and left to dry at room temperature. As before, dried membranes were heat-treated at 120 °C for 1 h for crosslinking.

2.4. Batch Reactions

Solketal levulinate reaction was carried out with PVA/SSA and PVA/SSA/ZIF-8 functional catalytic membranes at 105 °C. The loading of SSA acid catalyst in the catalytic membranes used in the reaction was 3, 6, 9 mmol and the initial molar ratios for Solketal/Levulinic Acid were chosen as 4/1, 5/1, 6/1. The batch reactor is shown in Figure 2.

ACCEPTED MANUSCRIPT

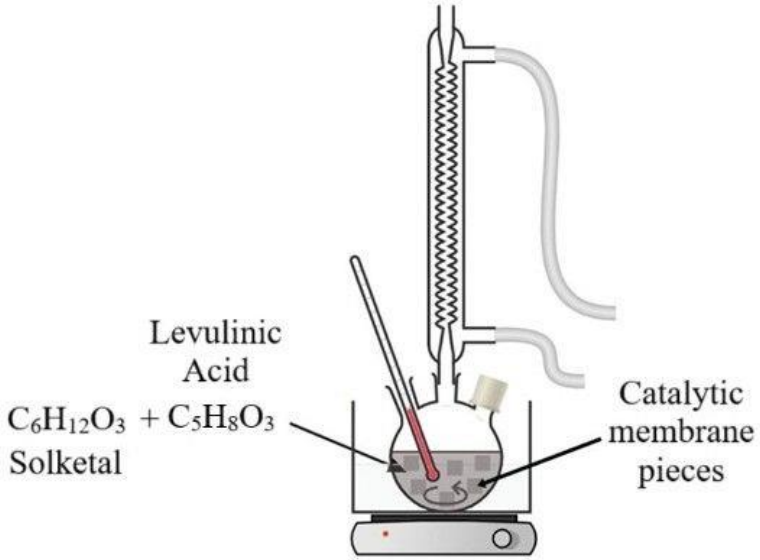

Fig. 2 Batch Reactor system

2.5. Analysis of Reaction Products

The catalytic performance of PVA/SSA and PVA/SSA/ZIF-8 functional catalytic membranes was analyzed by the titration method, with LA conversion calculated by Equation 1 (Unlu and Hilmioglu, 2016)

$$X=\frac{N_{Ao}-N_A}{N_{Ao}} \quad (1)$$

N_{Ao} is the number of moles of levulinic acid in solution at the beginning, and N_A is the number of moles of levulinic acid at any given time.

3. Results and Discussions

3.1. Fourier-transform infrared spectroscopy (FTIR) characterization of PVA/SSA and PVA/SSA/ZIF-8 catalytic Membranes

Fig. 3 shows the FTIR spectra of pure PVA, PVA/SSA, and PVA/SSA/ZIF-8 functional catalytic membranes. The characteristic peak observed at 3260 cm^{-1} wavenumber in pure PVA belongs to the O-H stretching band, while the characteristic absorbance peak at 1096 cm^{-1} is due to the C-O

ACCEPTED MANUSCRIPT

stretching (Khatuaa et al., 2015; Norouzi et al., 2021). When PVA/SSA functional catalytic membranes were examined, the O-H stretching band observed at 3260 cm^{-1} shifted to 3365 cm^{-1} upon addition of SSA to the structure. (Rynkowska et al., 2019). The peak observed at a wavelength of 1035 cm^{-1} is associated with the stretching vibration of the S-O bond, indicating the presence of SSA. 1725 cm^{-1} represents the C=O bond of SSA (Ngo et al., 2022). For PVA/SSA/ZIF-8, when ZIF-8 was added to the polymer matrix, it was observed that the peak intensity of the hydroxyl groups in the structure decreased. This can be explained by the high hydrophobicity of ZIF-8 (Yang et al., 2021).

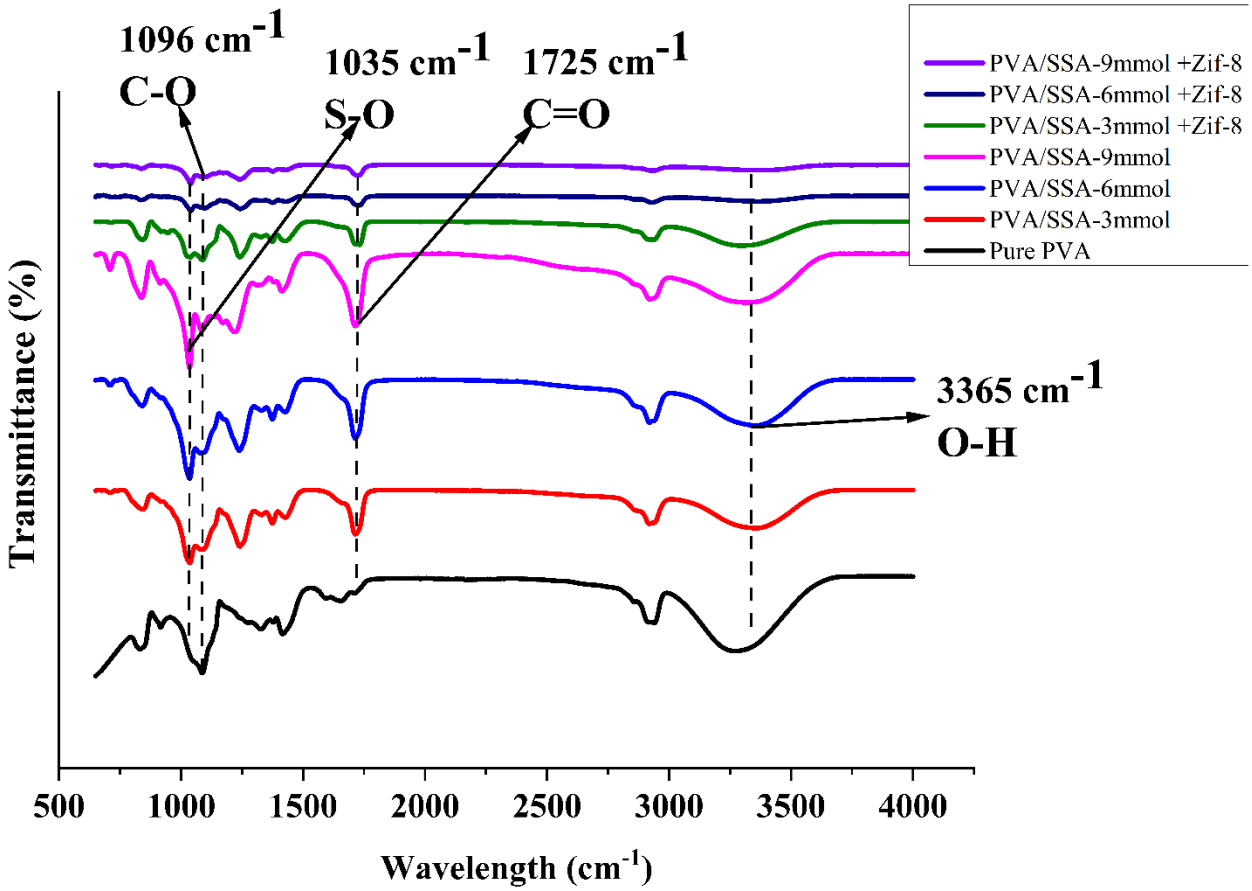

Fig. 3 FT-IR of PVA/SSA and PVA/SSA/ZIF-8 catalytic membranes

3.2. Thermogravimetric analysis (TGA) of PVA/SSA and PVA/SSA/ZIF-8 catalytic membranes

Three degradation regions were observed in the TGA curves of PVA/SSA and PVA/SSA/ZIF-8 catalytic membranes, shown in Fig. 4. While the first degradation in the 100°C-210°C temperature

range is due to the elimination of water in the structure, the degradation in the second region from 210°C to 300°C is related to the detachment of sulfonic groups from the ester bonds between SSA and PVA. The polymer chain decomposed in the last region (between 420 °C and 500 °C) (Gomaa et al., 2017; Maarouf et al., 2020). According to the TGA curves for PVA/SSA catalytic membranes, SSA added to PVA increased the thermal stability compared to pure PVA. In addition, the amount of residue at the end of the analysis increased directly with the amount of SSA (Rynkowska et al., 2019). No significant effect of ZIF-8 on thermal stability was observed.

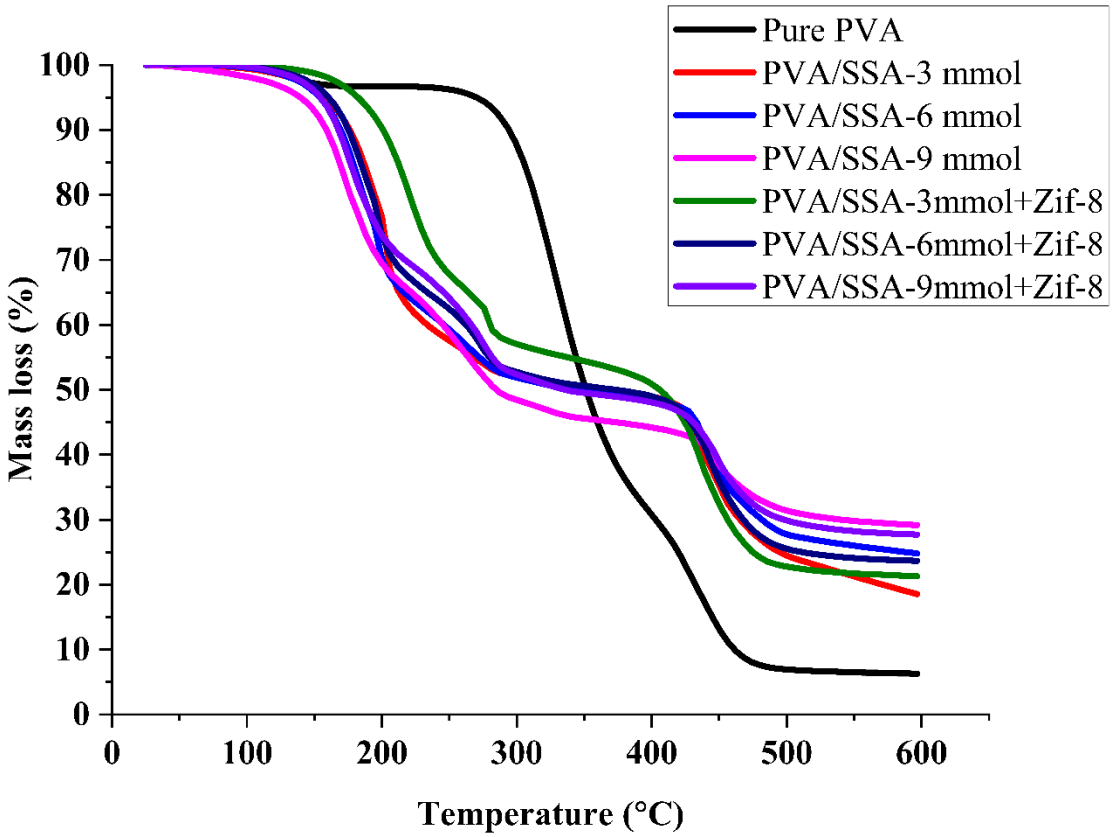

Fig. 4 TGA of PVA/SSA and PVA/SSA/ZIF-8 catalytic membranes

3.3. Scanning Electron Microscopy (SEM) and X-Ray Diffraction Analysis (XRD) Analyses of Synthesized ZIF-8

SEM image of the produced ZIF-8 is shown in Fig. 5. The SEM image of ZIF-8 is similar to the images in other studies in the literature (Attwa et al., 2024). The morphology of ZIF-8 contains

spherical ZIF-8 crystals (Thi Thanh et al., 2017). XRD peaks of produced ZIF-8 are shown in Fig. 6. The high-intensity diffraction peak at 2θ = 7.36 is an important characteristic peak of ZIF-8, indicating its high crystallinity (Qiu et al., 2022; Thi Thanh et al., 2017; Nordin et al., 2017).

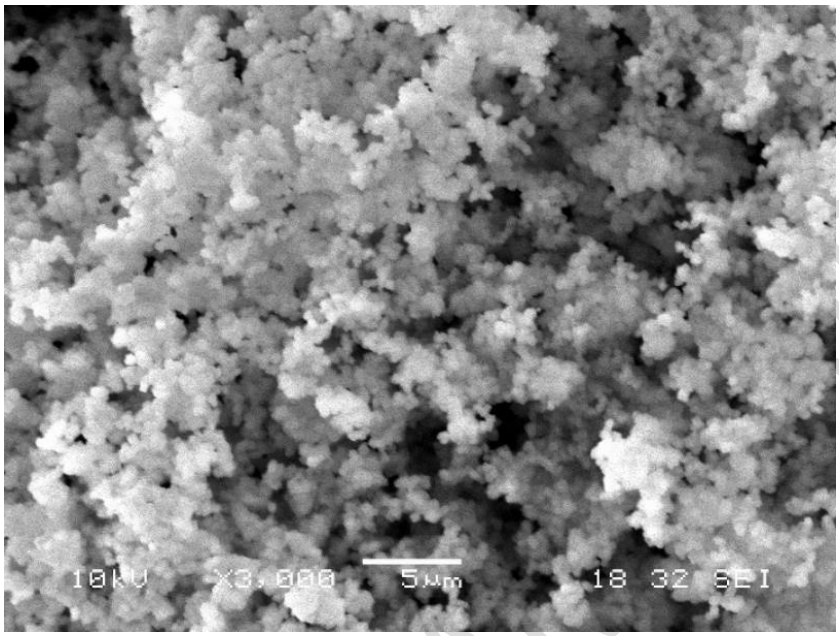

Fig.5 SEM image of ZIF-8 Crystals

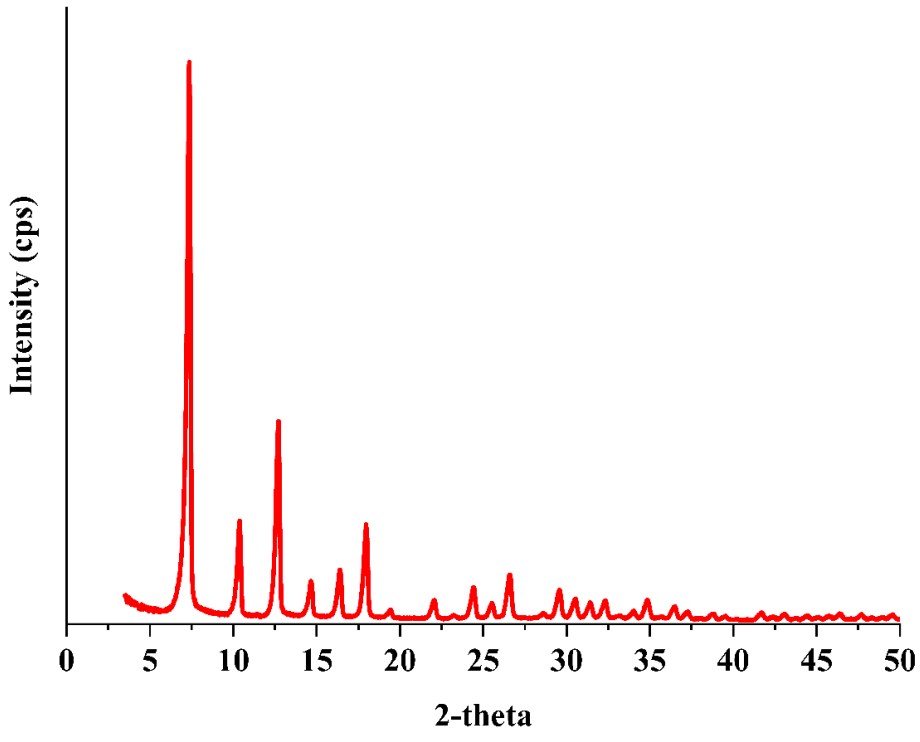

Fig. 6 XRD of ZIF-8

3.4. BET Analysis of ZIF-8

Table 1 shows the results of the BET analysis of ZIF-8.

Table 1. N_2 Adsorption/Desorption Data for the MOF of ZIF-8

Adsorbent (MOF ZIF-8)	
S_{BET} (m^2/g)	1831.70
Total Pore Volume (V_p (cm^3/g))	0.67
Average Pore Size (Å)	14.55
BJH Adsorption Pore Diameter (Å)	49.54
BJH Desorption Pore Diameter ()	38.93
HK Method Pore Diameter (Å)	4.32
SF Method Pore Diameter (Å)	6.18

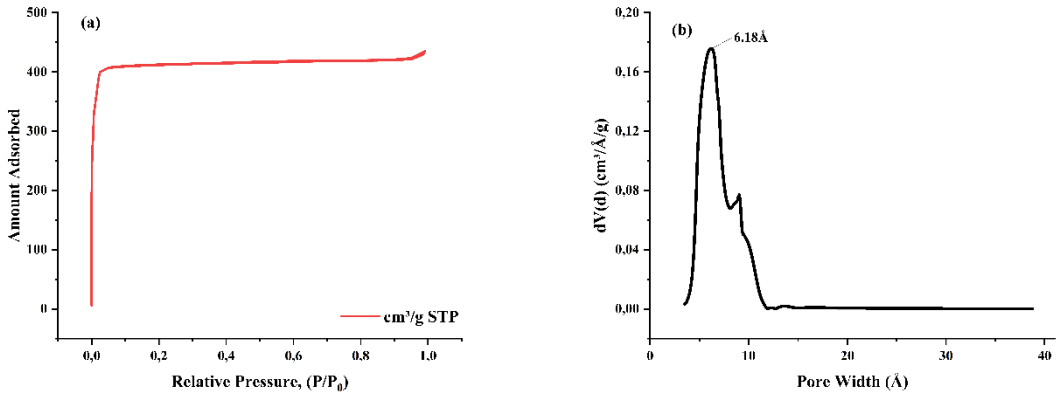

Fig. 7 (a) N_2 Adsorption/Desorption Isotherms Data for ZIF-8; (b) Pore Width(Å) for ZIF-8

Fig. 7 shows that ZIF-8 exhibits Type I isotherms according to the IUPAC classification. A significant increase in the amount adsorbed was observed at low P/P_0 values (0.015 P/P0 0.1). This result is typical for solid materials with microporous structures such as ZIF-8. According to the BET analysis, the specific surface area is 1831 m^2/g, the total pore volume at $P/P_0 = 0.99$ is 0.66 cm^3/g, and the pore size has a peak at 6.18 Å. Considering the range of 6.18 Å , where the peak is strongly observed, the pore size distribution shows that the material has a largely microporous structure. (Kruk and Jaroniec, 2001; Pan et. al.,2011; Missaoui et. al.,2022; Zhang et. al.,2022)

ACCEPTED MANUSCRIPT

3.5. Swelling Tests of PVA/SSA and PVA/SSA/ZIF-8 Catalytic Membranes

Swelling tests are performed to determine the affinity of a material for its solvent or reactants and products, if the material is to be used in a reaction medium. In this study, the synthesis of SoLE is an esterification reaction that releases water as a by-product. The presence of water in the reaction environment causes the reaction equilibrium to be directed to the side of the reactants, reducing the reaction yield. It is possible to shift the reaction towards product formation (Le Chatelier's Principle) by continuously removing water from the reaction medium (Liu and Ma, 2024; Zhu Jie et al., 2024). Therefore, the functional catalytic membrane must be hydrophilic. The water swelling results for the pure PVA, PVA/SSA, and PVA/SSA/ZIF-8 functional catalytic membranes used in the reaction are given in Tables 2 and 3. Water swelling rates were calculated with Equation (2).

$$\text{Swelling}(\%) = \frac{W_{wet} - W_{dry}}{W_{dry}} \text{x} 100 \quad (2)$$

In Equation 2; W_{wet} and W_{dry} signify wet catalytic membrane weight (g) and dry catalytic membrane weight (g), successively.

Table 2 Swelling tests of PVA/SSA catalytic membranes

Catalytic membrane	Swelling Rate (%)
Pure PVA	755.2
PVA/SSA-3 mmol	401.3
PVA/SSA-6 mmol	499.4
PVA/SSA-9 mmol	553.8

Table 2 shows that when SSA was added to PVA, the swelling rate decreased compared to pure PVA. The heat treatment after the addition of SSA reduced the swelling rate by cross-linking. As the amount of SSA in the catalytic membrane increased, the swelling ratios rose due to the increased number of hydrophilic sulfonic acid groups (Yagizatli et al., 2022). In Table 3, when ZIF-8 was added to the

ACCEPTED MANUSCRIPT

PVA/SSA catalytic membrane structure, a decrease in the swelling ratio was observed due to the hydrophobic effect of ZIF-8. (Sann et al., 2018).

Table 3 Swelling tests PVA/SSA/ZIF-8 catalytic membranes

Catalytic membrane	Swelling Rate (%)
Pure PVA	755.2
PVA/SSA-3 mmol+ZIF-8	381.5
PVA/SSA-6 mmol+ZIF-8	419.7
PVA/SSA-9 mmol+ZIF-8	483.1

3.6. Contact Angle Testing

In this study, esterification reaction was carried out with solketal and levulinic acid as reactants and solketal levulinate was obtained as product. However, the accumulation of water as a by-product in the reaction medium will reduce the product yield/reaction conversion and needs to be removed. Therefore, for the preparation of the catalytic membrane used in the reaction, PVA polymer, which is highly hydrophilic, thermally and chemically stable and environmentally friendly thanks to the hydroxyl groups it contains, was chosen; hydrophilicity or hydrophobicity in a material is explained as the ability of the selected material to bind to water molecules with hydrogen bonds on the part of its surface in contact with water ((Li W. et. al., 2013; Rezaee et. al., 2015; Yadav D. et. al., 2022). Water was used in the contact angle test to understand the hydrophilicity of the prepared membranes. When the liquid makes an angle of less than 90° with the contact surface, it indicates hydrophilicity, while an angle of more than 90° indicates hydrophobicity (Milne A. J. B. and Amirfazli A., 2009).

Zeolitic imidazolate frameworks (ZIFs), a subfamily of MOFs, are materials with the ability to tune their pore size and high chemical functionality while ZIF-8s are a new type with zeolite topology and have excellent chemical stability and high structural diversity found in all zeolite varieties. Its high chemical properties and thermally stable behavior indicate that it can be easily recycled from its

ACCEPTED MANUSCRIPT

environment in the process of use. ZIF-8 has a large surface area, strong and high degree of hydrophobicity (145°) and superoleophilic properties(San E. E. et. al.,2018; Zhang K. et. al.,2013).

Hydrophobicity/Hydrophilicity property is shown in Fig. 8 with contact angle values.

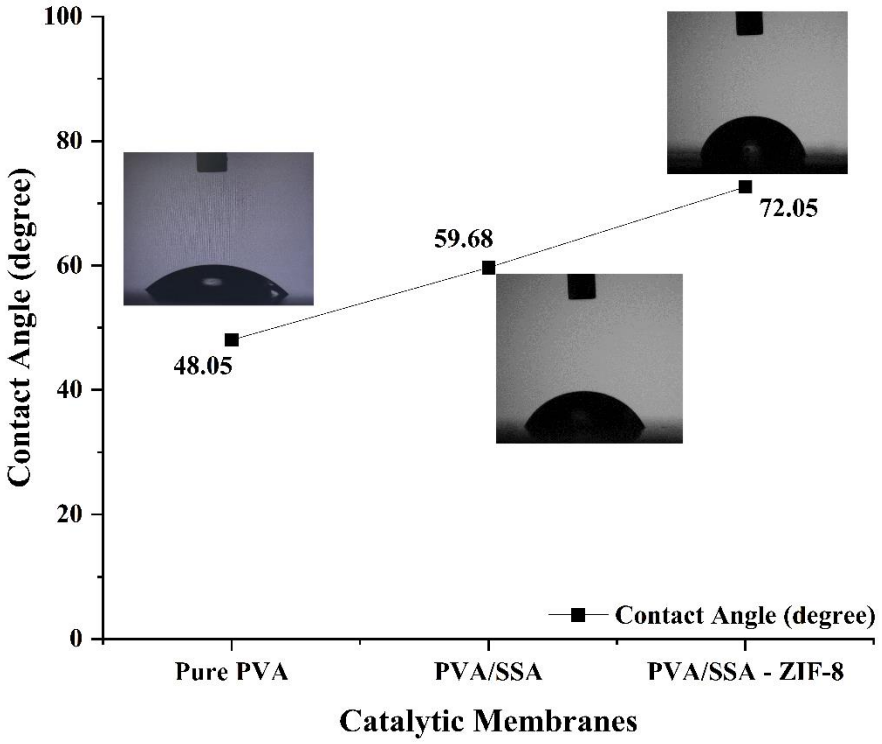

Fig 8. Contact Angles Degree of Pure PVA, PVA/SSA and PVA/SSA – ZIF-8

The addition of ZIF-8, which has high hydrophobicity, to the prepared PVA-based catalytic membrane brought the PVA polymer, which has high hydrophilicity, closer to its hydrophobicity. It is predicted that this gain in the catalytic membrane will provide energy efficiency by reducing the reaction time.

3.7. Interaction Parameters of PVA/SSA Catalytic membranes

The interaction between the by-product water and the polymer matrix of the catalytic membrane is well explained by the Flory-Huggins interaction parameter calculations. The Flory-Huggins interaction parameter helps to explain the interaction between a solvent and a polymer, based the amount of liquid sorbed by the polymer. As the interaction parameter approaches zero, the affinity of

ACCEPTED

the polymer for the solvent increases (Nistane et al., 2022). The interaction parameters for each SSA amount were calculated by Equations 3, 4, and 5.

$$\Phi_s = \frac{\frac{Q}{\rho_s}}{\frac{Q}{\rho_s} + \frac{1}{\rho_p}} \quad (3)$$

$$\Phi_p = 1 - \Phi_s \quad (4)$$

$$X_{ip} = -\frac{\ln(1-\Phi_p) + \Phi_p}{\Phi_p^2} \quad (5)$$

Here, Xip is the interaction parameter and dimensionless; Q (g/g) is the weight of water sorbed by one gram of polymeric membrane; ρs (g/cm^3) and ρp (g/cm^3) are densities of water and polymer, respectively. Φ_p and Φ_s are volume fractions of polymer and water, respectively. (Huang, 1991). The interaction parameters calculated for PVA/SSA catalytic membranes are shown in Table 4. A decrease in the values of the interaction parameters was observed as a result of increasing hydrophilicity with increasing number of hydrophilic sulfonic acid groups (Hasirci et al., 2023; Ohtake et al., 2022).

Table 4 Interaction parameters of PVA/SSA catalytic membranes

Catalytic membrane	**Interaction parameter**
PVA/SSA-3 mmol	0.521
PVA/SSA-6 mmol	0.486
PVA/SSA-9 mmol	0.439

ACCEPTED MANUSCRIPT

3.8. Acidity of PVA/SSA and PVA/SSA - ZIF-8 Catalytic Membranes

The acidic or basic properties of catalysts can be explained by the amount of H^+ / OH^- ions in their chemical structure. Although there are different methods in the literature, the most widely used method for determining the amount of acid/base is the ion displacement reaction.

Ion displacement reaction is determined by classical acid-base titration to determine the degree of acidity of a material depending on the acid groups it has. This is done as follows; a certain amount of the material whose acidity is to be determined is taken and kept in 1M NaCI solution for 48 hours. The H+ ions, which are replaced by Na+ ions in the salt solution, are titrated with 0.05 M NaOH together with phenolphthalein, which is prepared before titration and acts as an indicator (Atkar A. et al.,2024). Ion exchange capacity is calculated by Equation 6:

$$IDR\ (mmol\ H^+\ g^{-1}) = \frac{Consumption\ NaOH\ (ml) x NaOH\ Molarite}{Sample\ Weight} \quad (6)$$

Calculated ion displacements are given in Table 5.

Table 5. Acidity of PVA/SSA and PVA/SSA - ZIF-8 Catalytic Membranes

	ACIDITY (mmol H^+ g^{-1})
PVA - (w/w) 3mmol SSA	15.23
PVA - (w/w) 6mmol SSA	>16
PVA - (w/w) 9mmol SSA	>18
PVA - (w/w) 3mmol SSA/ZIF-8	15.24
PVA - (w/w) 6mmol SSA/ZIF-8	>16
PVA - (w/w) 9mmol SSA/ZIF-8	>18

Acidity values were also given in Fig. 9.

ACCEPTED MANUSCRIPT

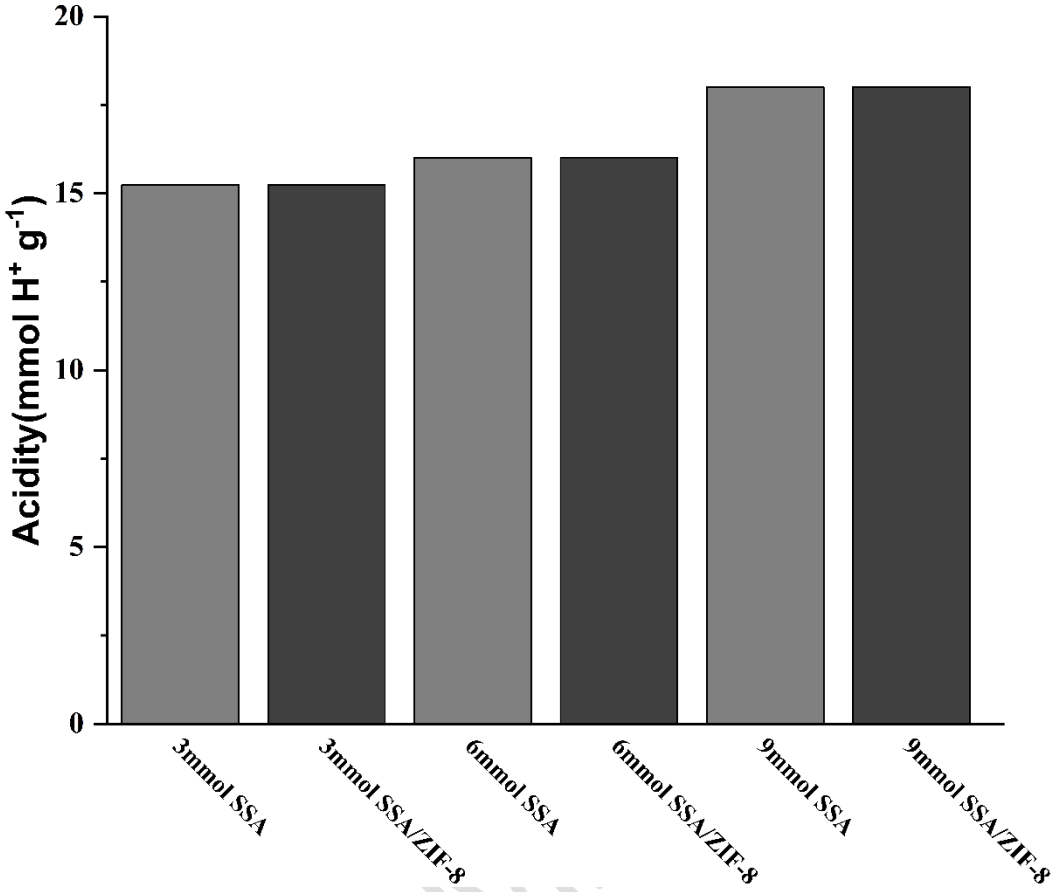

Fig 9. Acidity of PVA/SSA and PVA/SSA - ZIF-8 Catalytic Membranes

3.9. Batch Reactions with PVA/SSA and PVA/SSA/ZIF-8 Catalytic Membranes

Batch reactions with PVA/SSA and PVA/SSA/ZIF-8 catalytic membranes were performed at 105 °C and 3, 6, and 9 mmol SSA loadings, with Solketal/LA: 4/1, 5/1, 6/1 molar ratios. The effect of reaction time, SSA loading, and Solketal/LA ratio on reaction conversion was examined in batch reactions.

3.9.1 Influence of the reaction time on LA conversion

The influence of reaction time on the reaction conversion in the SoLE synthesis with PVA/SSA catalytic membranes at 9 mmol catalyst loading, with Solketal/LA: 6/1, and a reaction temperature of 105°C is given in Fig. 10. In the reaction carried out over the course of 8 hours, the conversion increased from 9.39% in the 1st hour to 97.65% in the 6th hour, where it reached a maximum. After

ACCEPTED M

6 hours, small decreases in reaction conversion were observed. Since the SoLE synthesis is a reversible reaction, after the 6th hour, the reaction may begin to favor the reactants' side due to the increasing amount of water as a by-product. Therefore, the optimum reaction time was determined to be 6 hours. (Chansorn et al., 2022; Zhang et al., 2021; Zhu Jishen et al., 2024).

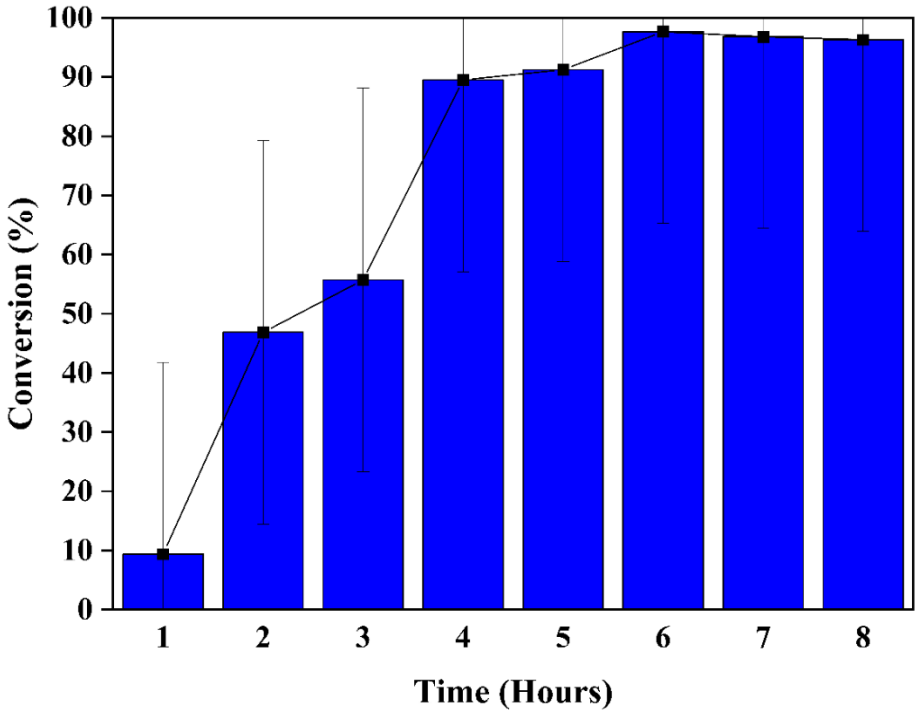

Fig 10. Influence of the reaction time on conversion with PVA/SSA catalytic membranes

To determine the optimized reaction time, SoLE synthesis was carried out with ZIF-8 doped PVA/SSA catalytic membranes at 9 mmol SSA loading, M:6/1 ratio, and 105 °C. As shown in Fig. 11, the reaction conversion increased from 38.01% at 1 hour to 96.81% at 4 hours. After 4 hours, no significant change in reaction conversion was observed. After 4 hours, the reaction reached an equilibrium state, and there was no significant change in conversion. The hydrophobicity of ZIF-8 prevented the occurrence of the reverse reaction. (Cao et al., 2021; Li et al., 2023). The optimum reaction time was determined to be 4 hours. The addition of ZIF-8 reduced the reaction time.

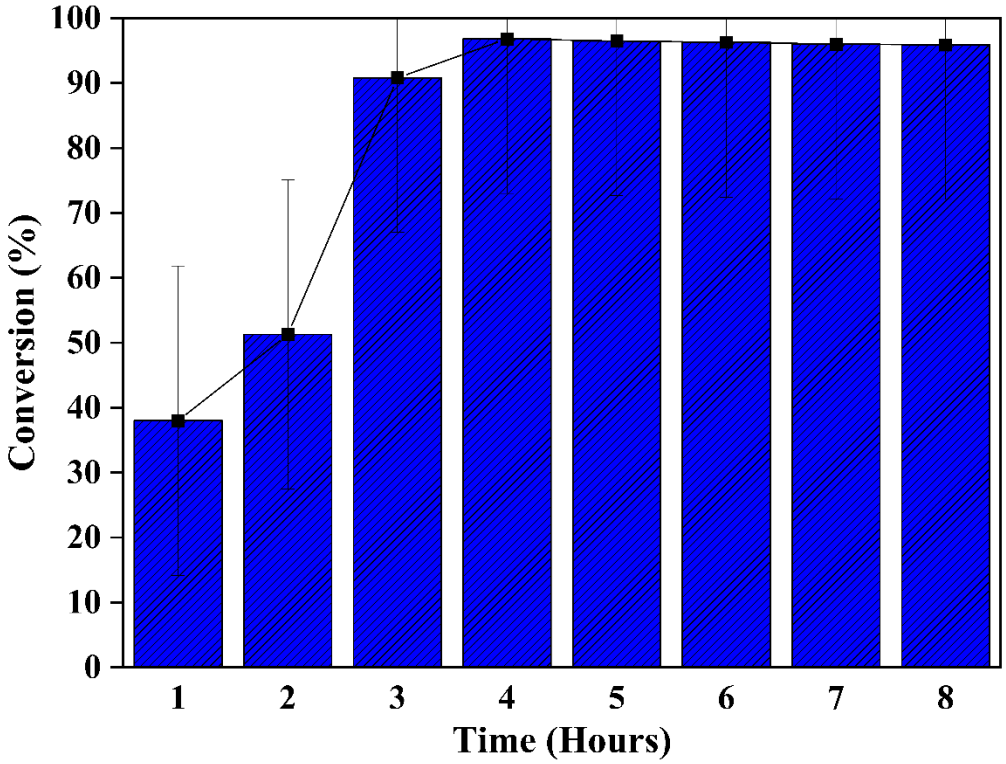

Fig 11. Influence of the reaction time on conversion with PVA/SSA/ZIF-8 catalytic membranes

Hydrophobic catalysts show high resistance to water. Since esterification reactions are reversible and limited by thermodynamic equilibrium, the hydrophobicity of the catalysts to be used allows the reacting organic molecules to adhere to the catalyst surface, while the desorption of by-product water molecules in esterification reactions and the selection of reactants in the reaction medium accelerate the reaction in the direction of the entrants and accelerate the ester formation (Liu, J. et. al., 2022). For this reason, they are often preferred for their ability to provide favorable conditions for reactants in esterification reactions. (Ristiana D. D. et. al., 2022; Suryandari A. S. et. al., 2023)

3.9.2 Influence of SSA loading on LA Conversion

The effect of SSA loading in the PVA/SSA catalytic membrane on LA conversion at 105°C and a 6/1 Solketal/LA ratio for 6 hours is presented in Fig. 12. The reaction conversion increased from 61.39% at 3 mmol SSA loading to 97.65% at 9 mmol SSA loading. Since the number of catalytically active sites in the membrane increased with increasing catalyst loading, an enhancement in reaction

ACCEPTED MA

conversion was observed (Zhang et al., 2024; Goda et al., 2022). However, a minimal difference was observed in terms of reaction conversion at 6 mmol and 9 mmol SSA loading.

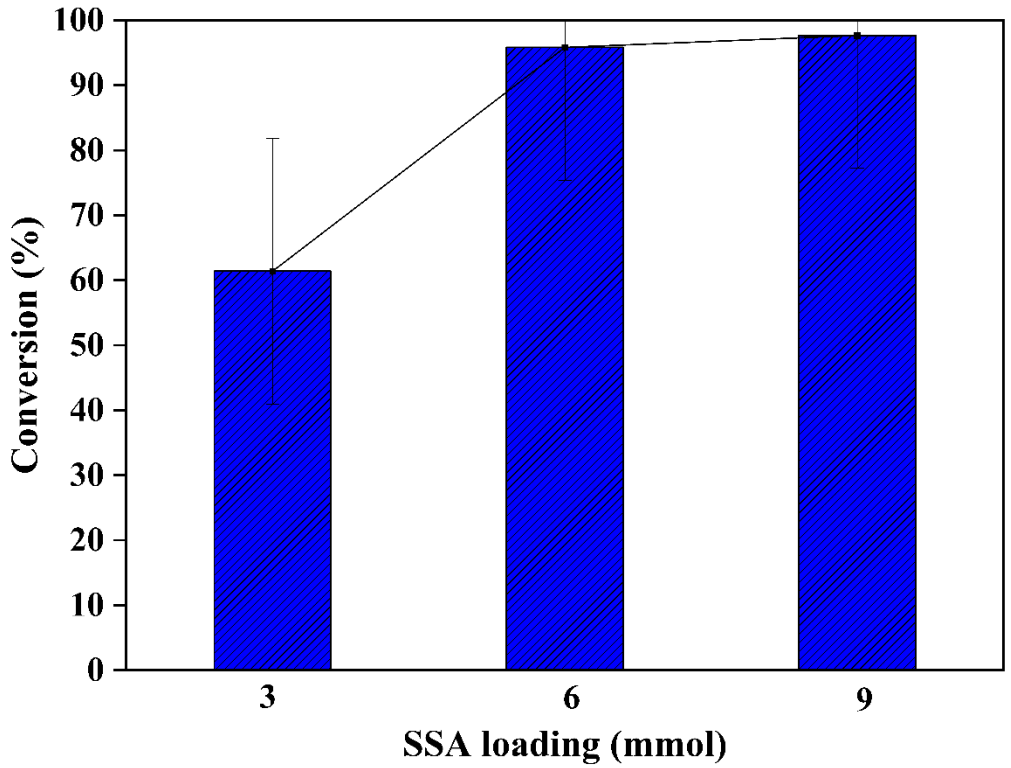

Fig. 12 Influence of SSA loading on conversion with PVA/SSA catalytic membranes

At 105 °C and with a ratio of M to 6/1, reactions were performed for 4 hours to observe the effect of the amount of catalyst on the reaction conversion in ZIF-8 doped PVA/SSA membrane. Fig. 13 shows that while 8.75% conversion was obtained at 3 mmol SSA catalyst loading, dramatic increases to conversion rates of 95.06% and 96.81% were obtained when the amount of catalyst was raised to 6 mmol and 9 mmol, respectively. No significant increase in reaction conversion was observed when SSA loading was raised from 6 mmol to 9 mmol (Soltani et al., 2021; Al-Saadi et al., 2020).

ACCEPTED

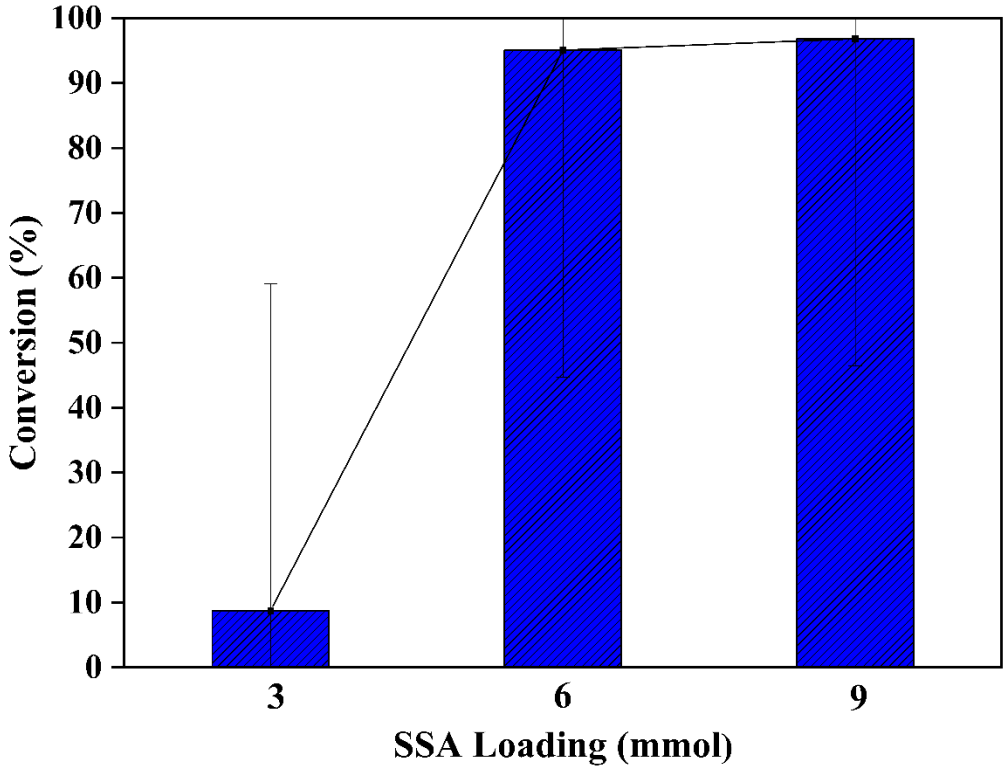

Fig. 13 Influence of SSA loading on conversion with PVA/SSA/ZIF-8 catalytic membranes

3.9.3 Influence of Solketal/LA initial molar ratio

To observe the effect of Solketal/LA molar ratio on the conversion with PVA/SSA catalytic membranes, the reactions were carried out at 105°C at a catalyst loading of 9 mmol for 6 hours, as shown in Fig. 14. At the molar ratios examined, very high conversions were obtained with very small differences in yields. While 95.26% conversion was obtained at M 4 to 1 ratio, conversion reached 97.65% at M 6 to 1 ratio. In the synthesis of SoLE (a reversible esterification reaction), feeding excess solketal, into the reaction medium can increase reaction conversion by shifting the balance towards product formation (Guo et al., 2021). However, the concentrations of the reactants and the conversion of the reaction may decrease due to the increasing amount of water, leading to a back reaction. (Cao et al., 2021). Thus, for the given molar ratios, increasing the Solketal/LA molar ratio did not cause a significant increase in the reaction conversion. The optimum molar ratio was determined as 4:1.

ACCEPTED MA

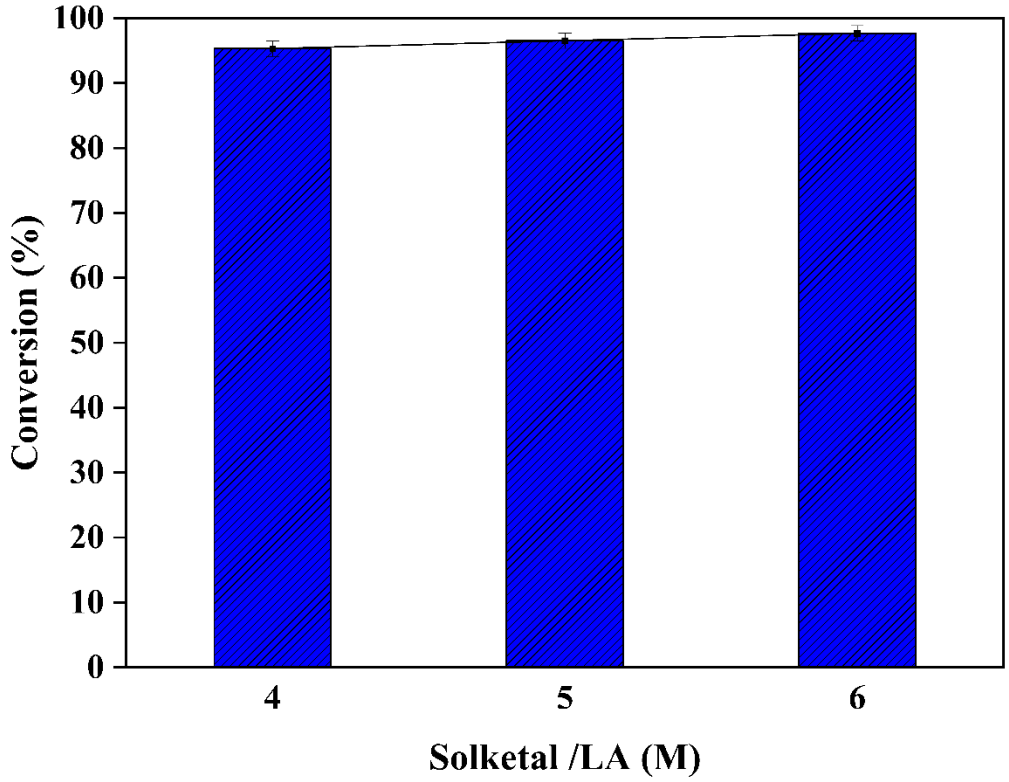

353

354 **Fig. 14** Influence of Solketal/LA molar ratio on conversion with PVA/SSA catalytic membranes

355 The effect of Solketal/LA molar ratios of 4/1, 5/1, and 6/1 on reaction conversion with PVA/SSA/ZIF-

356 8 catalytic membranes is shown in Fig. 15. The conditions of observation are 9 mmol catalyst loading,

357 a 105 °C reaction temperature, and a 4 h reaction time. The reaction conversion was 93.97% at M:4/1,

358 and reached 96.81% at M:6/1. The conversion data of the three different ratios were obtained very

359 close to each other, as shown in Fig. 12. At the given molar ratios, the reaction conversion has reached

360 the limit point (Mao et al., 2020). It was observed that the change in the determined molar ratios did

361 not significantly affect reaction conversion.

ACCEPTED MA

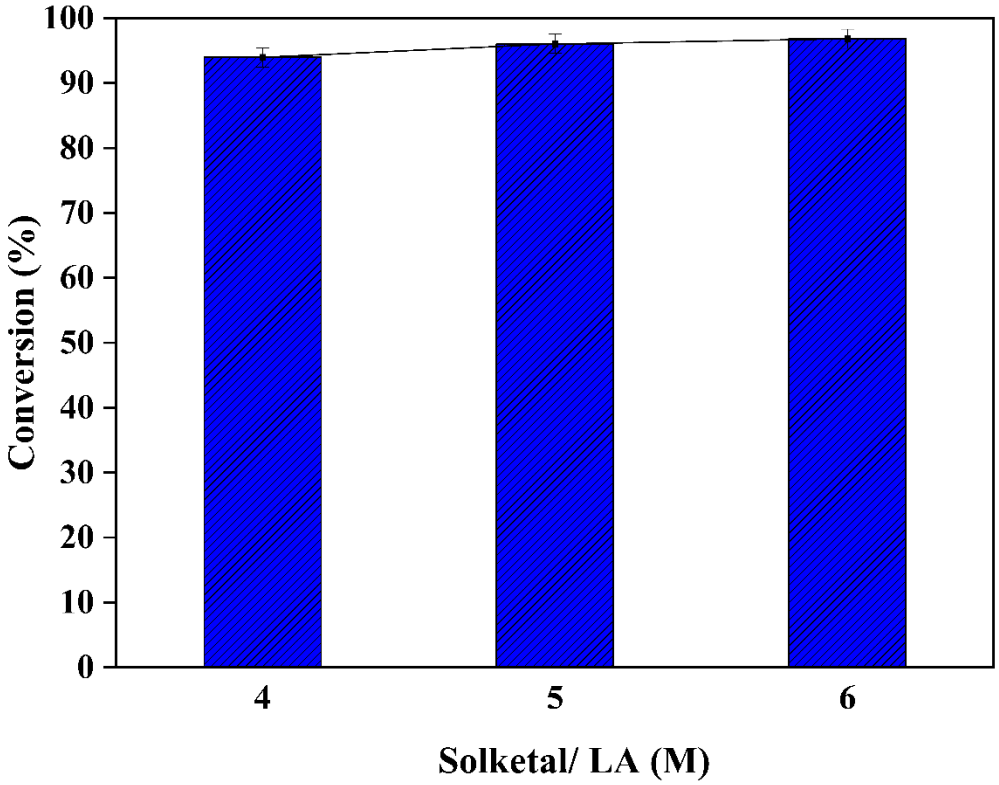

Fig. 15 Influence of Solketal/LA molar ratio on conversion with PVA/SSA/ZIF-8 catalytic membranes

4. Conclusions

In this study, a new generation of environmentally friendly fuel additive, solketal levulinate, was synthesized from the esterification of solketal and levulinic acid using functional PVA/SSA and PVA/SSA/ZIF-8 catalytic membranes in a batch reactor under mild conditions for the first time in the literature. Functional catalytic membranes were produced from a PVA matrix, SSA as a catalyst, and ZIF-8, a type of MOF, as a support material. The peak (S-O bond) at 1035 cm^{-1} in the FTIR analysis of the produced catalytic PVA/SSA membranes confirms the SSA loading. In addition, the presence of ZIF-8 in the PVA/SSA/ZIF-8 catalytic membrane structure increased the hydrophobicity of the structure. In TGA analysis, the integration of SSA to the PVA matrix increased the thermal stability. In swelling tests in water, SSA increased the hydrophilicity of the structure by increasing the extent of swelling. The catalytic membrane's ability to absorb water increases with an increasing swelling rate, thereby increasing the sorption support. The increased hydrophilicity of the catalytic membrane

with increasing SSA was supported by interaction parameter values approaching zero. The image of synthesized ZIF-8 crystals obtained by SEM was consistent with the literature. The high crystallinity of ZIF-8 crystals was determined by XRD analysis. The LA conversion obtained in SoLE production with a PVA/SSA functional catalytic membrane at 9 mmol catalyst loading, 105 °C, Solketal/LA molar ratio of 6/1, and a reaction time of 6 hours was **97.65%,** while the reaction conversion was 96.81% in SoLE synthesis with a PVA/SSA/ZIF-8 catalytic membrane under the same catalyst loading, temperature, and molar ratio, but with a reaction time of 4 hours. In this reaction, MOF ZIF-8 significantly reduced the reaction time, an improvement that cannot be ignored in terms of system cost. The developed functional catalytic membranes are promising and effective materials for the potential fuel additive SoLE synthesis**.**

Statements And Declarations

Competing Interests: The authors declare no conflict of interest.

Acknowledgement

This study was supported by the scientific research projects unit of Kocaeli University. Project No: FDK 2023-3201. Additionally, the authors would like to thank Guler Hasirci for her assistance in the preparation of the article.

References

Al-Saadi A., Mathan B., He Y. (2020), Esterification and transesterification over SrO–ZnO/Al_2O_3 as a novel bifunctional catalyst for biodiesel production, *Renewable Energy*, 158, 388–399, dx.doi.org/10.1016/j.renene.2020.05.171

Portillo Perez G. A., Pandey S., Dupont M. J. (2023), Sulfosuccinic acid-based metal-center catalysts for the synthesis of HMF from carbohydrates, *Catalysis Today*, 418, 1–11, dx.doi.org/10.1016/j.cattod.2023.114127

Mariam N. N. S., Hoong S.S., Maznee T. N., Arniza M. Z., Yusop R. M. (2024), Solketal Levulinate

ACCEPTED MANUSCRIPT

Ester as a Potential Fuel Addıtive For Palm Biodiesel, *Journal of Oil Palm Research*, 36, 104–114, dx.doi.org/10.21894/jopr.2023.0004

Attwa M., Said A., ElGamal M., El-Shaer Y., Elbasuney S. (2024), Bespoke Energetic Zeolite Imidazolate Frameworks-8 (ZIF-8)/Ammonium Perchlorate Nanocomposite: A Novel Reactive Catalyzed High Energy Dense Material with Superior Decomposition Kinetics, *Journal of Inorganic and Organometallic Polymers and Materials*, 34, 387–400, dx.doi.org/10.1007/s10904-023-02834-2

Çakmak A., Özcan H. (2018), Benzin İçin Oksijenli Yakıt Katkıları, *Journal of Polytechnic,* 0900, 831–840, dx.doi.org/10.2339/politeknik.457956

Cao M., Peng L., Xie Q., Xing K., Lu M., Ji J. (2021), Sulfonated Sargassum horneri carbon as solid acid catalyst to produce biodiesel via esterification, *Bioresource Technology,* 324, 124614, dx.doi.org/10.1016/j.biortech.2020.124614

Chansorn N., Amnuaypanich S., Soontaranon S., Rugmai S., Amnuaypanich S. (2022), Increasing solketal production from the solventless ketalization of glycerol catalyzed by nanodispersed phosphotungstic acid in poly(N-methyl-4-vinylpyridinium) grafted on silica nanoparticles, *Journal of Industrial and Engineering Chemistry*, 112, 233–243, dx.doi.org/10.1016/j.jiec.2022.05.017

Demirbas A., Balubaid M.A., Basahel A.M., Ahmad W., Sheikh M.H. (2015), Octane Rating of Gasoline and Octane Booster Additives, *Petroleum Science and Technology,* 33, 1190–1197, dx.doi.org/10.1080/10916466.2015.1050506

Doan T. D., Vu N. N., Hoang T. L. G., Nguyen-tri P. (2025), Metal-organic framework (MOF) - based materials for photocatalytic antibacterial applications, *Coord. Chem. Rev.*, 523, 216298, dx.doi.org/10.1016/j.ccr.2024.216298

Ethiraj J., Wagh D., Manyar H. (2022), Advances in Upgrading Biomass to Biofuels and Oxygenated Fuel Additives Using Metal Oxide Catalysts, *Energy and Fuels*, 36, 1189–1204,

ACCEPTED MANUSCRIPT

426 dx.doi.org/10.1021/acs.energyfuels.1c03346

427 Fernández P., Fraile J.M., García-Bordejé E., Pires, E. (2019), Sulfonated hydrothermal carbons
428 from cellulose and glucose as catalysts for glycerol ketalization, *Catalysts*, 9, 804,
429 dx.doi.org/10.3390/catal9100804

430 Goda M.N., Said A.E.A.A., El-Aal M.A. (2022), Mineral acid-activated sugarcane bagasse ash as
431 solid acid catalyst for the liquid phase esterification of acetic acid with n-amyl, benzyl, and n-
432 butyl alcohols, *Journal of Environmental Chemical Engineering,* 10, 107355,
433 dx.doi.org/10.1016/j.jece.2022.107355

434 Gomaa M.M., Hugenschmidt C., Dickmann M., Abdel-Hamed M.O., Abdel-Hady E.E., Mohamed
435 H.F.M. (2017), Free volume of PVA/SSA proton exchange membrane studied by positron
436 annihilation lifetime spectroscopy, *Acta Physica Polonica A,* 132, 1519–1522,
437 dx.doi.org/10.12693/APhysPolA.132.1519

438 Guo M., Jiang W., Chen C., Qu S., Lu J., Yi W., Ding J. (2021), Process optimization of biodiesel
439 production from waste cooking oil by esterification of free fatty acids using La 3 + / ZnO-TiO_2
440 photocatalyst, *Energy Conversion and Management,* 229, 113745,
441 dx.doi.org/10.1016/j.enconman.2020.113745

442 Hasirci G., Ilgen O., Hilmioglu N. (2023), Synthesis of the Environmentally Friendly Fuel
443 Bioadditive Solketal by the Green Catalytic Membrane PVA/PAMPS, *Water, Air, & Soil*
444 *Pollution*, 234, 1–14, dx.doi.org/10.1007/s11270-023-06680-3

445 Hilmioglu N. (2022), Optimization of Synthesis of Ethyl Acetate by Response Surface Method and
446 Investigation of Reactive Sorption Effect of Hydrogel in Synthesis, *European Journal of Science*
447 *and Technology*, 35, 94–101, dx.doi.org/10.31590/ejosat.1061611

448 Huang R.Y.M. (1991), Pervaporation Membrane Sepration Processes. Membrane Science and
449 Technology, 1 st edition, New York.

ACCEPTED MANUSCRIPT

Ilgen O., Yerlikaya S., Akyurek F.O. (2017), Synthesis of Solketal from Glycerol and Acetone over Amberlyst-46 to Produce an Oxygenated Fuel Additive, *Periodica Polytechnica Chemical Engineering,* 61 (2), 144–148, dx.doi.org/10.3311/PPch.8895

Jeanmard L., Rongwong W., Chisti Y. (2025), Biomass and Bioenergy Biomass-derived levulinic acid as a platform chemical for making diverse products, *Biomass and Bioenergy*, 195, 107683, dx.doi.org/10.1016/j.biombioe.2025.107683

Jia S., Ma J., Wang D., Wang K., Zheng Q., Song C., Guo X. (2020), Fast and efficient upgrading of levulinic acid into long-chain alkyl levulinate fuel additives with a tungsten salt catalyst at low temperature, *Sustainable Energy & Fuels*, 4, 2018–2025, dx.doi.org/10.1039/c9se01287g

Khatuaa C., Chinyaa I., Sahab D., Dasa S., Sena R., Dhara A. (2015), Modified clad optical fibre coated with PVA/TiO_2 nano composite for humidity sensing application, *International Journal on Smart Sensing and Intelligent Systems*, 8, 1424–1442, dx.doi.org/10.21307/ijssis-2017-813

Laeim H., Molahalli V., Prajongthat P., Pattanaporkratana A., Pathak G., Phettong B., Hongkarnjanakul N., Chattham N. (2025), Porosity Tunable Metal-Organic Framework (MOF) -Based Composites for Energy Storage Applications : Recent Progress, *Polymers*, 17, 130, dx.doi.org/10.3390/polym17020130

Li Y., Zhu K., Jiang Y., Chen L., Zhang H., Li H., Yang S. (2023), Biomass-derived hydrophobic metal-organic frameworks solid acid for green efficient catalytic esterification of oleic acid at low temperatures, *Fuel Processing Technology*, 239, 107558, dx.doi.org/10.1016/j.fuproc.2022.107558

Liu H., Ma Z., Liu X., Wu Y., Zhang W., Zhao S. (2024), Green synthesis of biobased glycerol levulinate ketal in a continuous flow reactor : Optimization, kinetics and simulation, *Applied Energy,* 361, 122910, dx.doi.org/10.1016/j.apenergy.2024.122910

Liu Z., Ma Y. (2024), Chemical Recycling of Step-Growth Polymers Guided by Le Chatelier's

ACCEPTED MANUSCRIPT

Principle, *ACS Engineering Au,* 4, 432-449, dx.doi.org/10.1021/acsengineeringau.4c00015

Maarouf S., Alouane Z., Tazi B., Guenoun F., Fouad K. (2020), Fabrication and properties of hybrid membranes based on poly (vinyl alcohol), sulfosuccinic acid and salts of heteropolyacid with or without silica for fuel cells applications, *Advances in Science, Technology and Engineering Systems*, 5, 1013–1019, dx.doi.org/10.25046/aj0505124

Mao F.F., Zhao W., Tao D.J., Liu X. (2020), Highly Efficient Conversion of Renewable Levulinic Acid to n-Butyl Levulinate Catalyzed by Sulfonated Magnetic Titanium Dioxide Nanotubes, *Catalysis Letters*, 150, 2709–2715, dx.doi.org/10.1007/s10562-020-03177-0

Moradi P., Saidi M., Najafabadi A.T. (2021), Biodiesel production via esterification of oleic acid as a representative of free fatty acid using electrolysis technique as a novel approach : Non-catalytic and catalytic conversion, *Process Safety and Environmental Protection*, 147, 684–692, dx.doi.org/10.1016/j.psep.2020.12.032

Mussatto S.I., Dragone G., Guimarães P.M.R., Silva J.P.A., Carneiro L.M., Roberto I.C., Vicente A., Domingues L., Teixeira J.A. (2010), Technological trends, global market, and challenges of bio-ethanol production, *Biotechnology Advances*, 28, 817–830, dx.doi.org/10.1016/j.biotechadv.2010.07.001

Ngo H.L., Nguyen N.T., Ho T.T.N., Pham H.V., Le T.N., Tran T.N., Huynh L.T.N., Pham T.N., Nguyen T.T., Nguyen T.H., Le V.H., Tran D.L. (2022), The performance of MCDI: the effect of sulfosuccinic acid ratio in the PVA-based cation exchange membrane, *Ionics*, 28, 4369–4380, dx.doi.org/10.1007/s11581-022-04661-w

Mariam N.N.S., Hoong S.S., Arniza M. Z., Adnan S., Ismail T. N. M. T., Yeong S. K., Yusop M. R. (2021), Optimisation Of Reaction Parameters For The Synthesis Of Solketal Levulinate As Potential Biodiesel Additive, *Journal of Oil Palm Research*, 34(3), 524-534, dx.doi.org/10.21894/jopr.2021.0052

ACCEPTED MANUSCRIPT

Nistane J., Chen L., Lee Y., Lively R., Ramprasad R. (2022), Estimation of the Flory-Huggins interaction parameter of polymer-solvent mixtures using machine learning, *MRS Communications*, 12, 1096–1102, dx.doi.org/10.1557/s43579-022-00237-x

Nordin N. A. H. M., Ismail A. F., Yahya N. (2017), Zeolitic imidazole framework 8 decorated graphene oxide (ZIF-8/GO) mixed matrix membrane (MMM) for CO_2/CH_4 separation, *Jurnal Teknologi-Sciences & Engineering*, 79, 59–63, doi.org/10.11113/jt.v79.10438

Norouzi M.A., Montazer M., Harifi T., Karimi P. (2021), Flower buds like PVA/ZnO composite nanofibers assembly: Antibacterial, in vivo wound healing, cytotoxicity and histological studies, *Polymer Testing*, 93, 106914, dx.doi.org/10.1016/j.polymertesting.2020.106914

Ohtake T., Ito H., Horiba K., Toyoda N. (2022), Synthesis of Water-Soluble Polymeric Surfactants Bearing Sulfonic Acid Groups and the Effects of Hydrophilic Components on the Rheology and Dispersive Properties of Dye Dispersions, *ACS Applied Polymer Materials*, 4, 8556–8563, dx.doi.org/10.1021/acsapm.2c01471

Pan Y., Liu Y., Zeng G., Zhao L., Lai Z. (2011), Rapid synthesis of zeolitic imidazolate framework-8 (ZIF-8) nanocrystals in an aqueous system, *Chemical Communications*, 47, 2071–2073, dx.doi.org/10.1039/C0CC05002D

Qiu K., Shu Y., Zhang J., Gao L., Xiao G. (2022), Effective and Stable Zeolite Imidazole Framework-Supported Copper Nanoparticles (Cu/ZIF-8) for Glycerol to Lactic Acid, *Catalysis Letters*, 152, 172–186, dx.doi.org/10.1007/s10562-021-03610-y

Wi´sniewska P., Haponiuk J., Saeb M, R., Rabiee N., Bencherif S. A. (2023), Mitigating metal-organic framework (MOF) toxicity for biomedical applications, *Chemical Engineering Journal*, 471, 144400, dx.doi.org/10.1016/j.cej.2023.144400

Rynkowska E., Fatyeyeva K., Kujawa J. (2019), Chemically and Thermally Crosslinked PVA-Based Membranes: Effect on Swelling and Transport Behavior, *Polymers,* 11, 1799,

ACCEPTED MANUSCRIPT

522 dx.doi.org/10.3390/polym11111799

523 Sajid M., Farooq U., Bary G., Azim M. M., Zhao X. (2021), Sustainable production of levulinic acid
524 and its derivatives for fuel additives and chemicals: progress, challenges, and prospects, *Green*
525 *Chemistry*, 23, 9198–9238, dx.doi.org/10.1039/d1gc02919c

526 Sann E. E., Pan Y., Gao Z., Zhan S., Xia F. (2018), Highly hydrophobic ZIF-8 particles and
527 application for oil-water separation, *Separation and Purification Technology*, 206, 186–191,
528 dx.doi.org/10.1016/j.seppur.2018.04.027

529 Singh P.K., Kumar S.S., Lakshmana Kumar S., Kulandaivel A., Geerthik S., Ganeshan P., Sathish
530 Kannan, S., Seikh, A.H., Iqbal A. (2023), Impact of oxy-additives on diesel engine performance
531 and emission parameters using waste cooking oil biodiesel, *Global NEST Journal*, 25, 105–112,
532 dx.doi.org/10.30955/gnj.004983

533 Soltani S., Khanian N., Shean T., Choong Y., Asim N., Zhao Y. (2021), Microwave-assisted
534 hydrothermal synthesis of sulfonated TiO 2 -GO core – shell solid spheres as heterogeneous
535 esterification mesoporous catalyst for biodiesel production, *Energy Conversion and*
536 *Management*, 238, 114165, dx.doi.org/10.1016/j.enconman.2021.114165

537 Song W., Zhao X., Jin Z., Fan L., Ji, X. (2023), Poly (vinyl alcohol) for multi-functionalized
538 corrosion protection of metals : A review, *Journal of Cleaner Production*, 394, 136390,
539 dx.doi.org/10.1016/j.jclepro.2023.136390

540 Sutinno, S. (2016), Esterification of Solketal And Levulinic Acid Over Heterogeneous Acid
541 Catalysts, Degree of Master Thesis, Petrochemistry and Polymer Science, Chulalongkorn
542 University.

543 Thanh M. T., Thien T. V., Chau V.T. T., Du P. D., Hung N. P., Khieu D. Q. (2017), Synthesis of Iron
544 Doped Zeolite Imidazolate Framework-8 and Its Remazol Deep Black RGB Dye Adsorption
545 Ability, *Journal of Chemistry*, 2017, 1-18, dx.doi.org/10.1155/2017/5045973

ACCEPTED MANUSCRIPT

546 Unlu D., Hilmioglu N. D. (2019), Production of Fuel Bioadditive “Triacetin” Using a
547 Phosphomolybdic-Acid-Loaded PVA Membrane in a Pervaporation Catalytic Membrane
548 Reactor, *Energy Fuels*, 33, 2208-2218, dx.doi.org/10.1021/acs.energyfuels.8b03344

549 Unlu D., Hilmioglu N. D. (2016), Environmental Effects Fuel bioadditive production by chitosan /
550 sulfosuccinic acid catalytic membrane, *Energy Sources, Part A: Recovery, Utilization, and*
551 *Environmental Effects*, 38, 3606–3611, dx.doi.org/10.1080/15567036.2016.1166166

552 Xu Y., Guo P., Chang C., Li P., Zhao S., Xu G. (2020), Aluminum chloride-catalyzed conversion of
553 levulinic acid to methyl levulinate: optimization and kinetics, *Journal of Chemical Technology*
554 *& Biotechnology,* 95, 2251–2260, dx.doi.org/10.1002/jctb.6413

555 Yagizatli Y., Sahin A., Ar I. (2022), Effect of thermal crosslinking process on membrane structure
556 and PEM fuel cell applications performed with SPEEK-PVA blend membranes, *International*
557 *Journal of Hydrogen Energy*, 47, 40445–40461, dx.doi.org/10.1016/j.ijhydene.2022.04.183

558 Yang F., Wu J., Zhu X., Ge T., Wang R. (2021), Enhanced stability and hydrophobicity of LiX@ZIF-
559 8 composite synthesized environmental friendly for CO_2 capture in highly humid flue gas,
560 *Chemistry Engineering Journal*, 410, 128322, dx.doi.org/10.1016/j.cej.2020.128322

561 Zhang B., Gao M., Geng J., Cheng Y., Wang X., Wu C., Wang Q., Liu S., Cheung S.M. (2021),
562 Catalytic performance and deactivation mechanism of a one-step sulfonated carbon-based solid-
563 acid catalyst in an esterification reaction, *Renewable Energy*, 164, 824–832,
564 dx.doi.org/10.1016/j.renene.2020.09.076

565 Zhang Q., Hong X., Lei J., Lei Y., Yang Y., Cheng J., Hu Y., Zhang Y. (2024), Environmentally-
566 friendly preparation of Sn(II)-BDC supported heteropolyacid as a stable and highly efficient
567 catalyst for esterification reaction, *Journal of Saudi Chemical Society,* 28, 101832,
568 dx.doi.org/10.1016/j.jscs.2024.101832

569 Zhu Jishen., Jiang W., Yuan Z., Lu J., Ding J. (2024), Taguchi method for optimizing the cation

ACCEPTED MANUSCRIPT

exchange resin catalyzed esterification of oleic acid with ethanol and adsorption kinetics study, *Process Safety and Environmental Protection*, 182, 989–998, dx.doi.org/10.1016/j.psep.2023.12.052

Zhu Jie., Li L., Cao M. (2024), Le Chatelier's principle to stabilize intrinsic surface structure of oxygen-evolving catalyst for enabling ultra-high catalytic stability of zinc-air battery and water splitting, *Nano Energy*, 122, 109300, dx.doi.org/10.1016/j.nanoen.2024.109300

Li W., Liu W., Xing W., Xu N. (2013), Esterification Of Acetic Acid And N-Propanol With Vapor Permeation Using NaA Zeolite Membrane, *Industrial And Engineering Chemistry Research*, 52, 6336−6342, dx.doi.org/10.1021/ie3031086

Rezaee R., Nasseri S., Mahvi A. H., Nabizadeh R., Mousavi S. A., Rashidi A., Jafari A., Nazmara S. (2015), Fabrication and characterization of a polysulfone-graphene oxide nanocomposite membrane for arsenate rejection from water, *Journal of Environmental Health Science and Engineering*, 213(61), dx.doi.org/10.1186/s40201-015-0217-8

Sann E. E., Pan Y., Gao Z., Zhan S., Xia F. (2018), Highly hydrophobic ZIF-8 particles and application for oil-water separation, *Separation and Purification Technology*, 206, 186–191.

Zhang K., Lively R. P., Zhang C., Chance R. R., Koros W. J., Sholl D. S., Nair S. (2013), Exploring the Framework Hydrophobicity and Flexibility of ZIF-8: From Biofuel Recovery to Hydrocarbon Separations, *The Journal of Physical Chemistry Letters*, 4, 3618−3622, dx.doi.org/10.1021/jz402019d.

Yadav D., Karunanithi A., Saxena S., Shukla S. (2022), Modified PVA membrane for separation of micro-emulsion, *Science of the Total Environment*, 822, 153610, dx.doi.org/10.1016/j.scitotenv.2022.153610

Milne A. J. B. and Amirfazli A. (2009), Drop Shedding by Shear Flow for Hydrophilic to Superhydrophobic Surfaces, *Langmuir*, 25(24), 14155–14164, dx.doi.org/10.1021/la901737y.

ACCEPTED MANUSCRIPT

Ristiana D. D., Suyanta S., Nuryono N. (2022), Sulfonic acid-functionalized silica with controlled hydrophobicity as an effective catalyst for esterification of levulinic acid, *Materials Today Communications*, 32, 103953, dx.doi.org/10.1016/j.mtcomm.2022.103953.

Liu, J., Shi, J., Zhang, B., Cheng, Z. (2022), Novel Magnetically- Recoverable Solid Acid Catalysts with a Hydrophobic Layer in Protecting the Active Sites from Water Poisoning, *Processes*, 10, 1738, dx.doi.org/10.3390/ pr10091738.

Suryandari A. S., Nurtono T., Widiyastuti W., Setyawan H. (2023), Hydrophobic Modification of Sulfonated Carbon Aerogels from Coir Fibers To Enhance Their Catalytic Performance for Esterification, *ACS Omega*, 8, 27139−27145, dx.doi.org/10.1021/acsomega.3c02244.

Atkar A., Bajad S. S. G., Deshmukh S., Dinker A., Kishor K. (2024), Synthesis and characterization of sulfonated chitosan (SCS) / sulfonated polyvinyl alcohol (SPVA) blend membrane for microbial fuel cell application, *Materials Science and Engineering B*, 299, 116942, dx. doi.org/10.1016/j.mseb.2023.116942

Kruk M., Jaroniec M., 2001, Gas Adsorption Characterization of Ordered Organic−Inorganic Nanocomposite Materials, Chemistry of Materials, 13, 10, 3169–3183, dx. doi.org/10.1021/cm0101069

Pan Y., Liu Y., Zeng G., Zhaoa L., Lai Z., 2011, Rapid synthesis of zeolitic imidazolate framework-8 (ZIF-8) nanocrystals in an aqueous system, Chemical Communication, 47, 2071-2073, dx. doi.org/10.1039/C0CC05002D

Missaoui N., Kahri H., Demirci U. B., 2022, "Rapid room-temperature synthesis and characterizations of high-surface-area nanoparticles of zeolitic imidazolate framework-8 (ZIF-8) for CO2 and CH4 adsorption", Journal of Materials Science, 57, 16245–16257, dx. doi.org/10.1007/s10853-022-07676-w

Zhang M., Ming J., Zhang W., Xie J., Lin P., Song X., Chen X., Wang X., Zhou B., 2022, Porous

ACCEPTED MANUSCRIPT

618 Organic Polymer-Derived Fe2P@N,P-Codoped Porous Carbon as Efficient Electrocatalysts for
619 pH Universal ORR, ACS Omega, 5, 7225−7234, dx. doi.org/10.1021/acsomega.2c00216

620

ACCEPTED MANUSCRIPT